Thermal Characteristics of Streaming Potential Mediated Flows of Non-Newtonian Fluids with Asymmetric Boundary Conditions and Steric Effect

Ritesh Agarwal[1], Nikhil Desai[1], Jeevanjyoti Chakraborty[2,3], Ranabir Dey[1] and Suman Chakraborty[1,2,*]

[1]Mechanical Engineering Department, IIT Kharagpur, West Bengal – 721302
[2]Advanced Technology Development Centre, IIT Kharagpur, West Bengal – 721302
[3]Current affiliation: Mathematical Institute, University of Oxford, Oxford OX2 6GG, United Kingdom

ABSTRACT

Electrokinetic flows through narrow confinements have mostly been studied with symmetric boundary conditions on the walls even though in practice it is very common to have these walls made of different materials which in turn lead to different surface charge conditions on them. Such a dearth of studies is particularly acute in streaming potential flows which are naturally predisposed to strongly influence even simple pressure-driven flows in such narrow confinements. Further, the very nature of the fluid may, in general cases, be of non-Newtonian nature; this is especially true for biomedical assays. Motivated by this, we address a model problem of a streaming potential mediated flow of a power-law fluid through a slit channel having different boundary conditions. Additionally, as an important new contribution to this line of investigation, we study the thermal characteristics of such flow. Noting, pertinently, that the streaming potential effects are especially stronger for high values of the surface charge (which translates into high magnitudes of the zeta potential), we present a general framework that incorporates steric effects of the ions. This is done to avoid the unphysical ionic distributions predicted by the traditional Boltzmann approximation.

1. INTRODUCTION

It can be intuitively followed that as we tend towards micro-scale fluid flow and heat transfer, surface effects become more prominent than volumetric effects. Out of all the surface effects, electrokinetic effects are one of the most prominent in microfluidics. Most solid surfaces tend to acquire a net surface charge in contact with polar medium; the most common mechanisms behind such charge generation are ionization of covalently bonded groups or ion absorption [1, 2]. Such charged surfaces are invariably accompanied by a distribution of ions in their vicinity. The ions that are charged oppositely to the charged surface are called counter-ions, and the ions that have the same charge polarity as the surface are called co-ions. The ionic distribution is established through an equilibrating interplay between the Coulombic forces and entropic interactions. The surface charge together with the ion distribution constitutes the electric double layer (EDL) [3, 4]. Very close to the wall there is an immobile layer of counter-ions, bonded strongly to the surface, called the Stern layer [3, 4]. The potential at the edge of the Stern layer is called zeta potential (ζ). We have taken into account different zeta potentials at both walls because in most of the lab-on-a-chip devices the micro flow confinements comprise two different materials, like PDMS and glass, or PMMA and glass [5]. Hence, for such flow conduits, it is more practical to assume different zeta potentials at the two walls. Now, when pressure-

*Corresponding author: suman@mech.iitkgp.ernet.in

driven ionic aqueous solution flows in the presence of a charge distribution as part of the EDL, ions are advected along with the fluid, causing a streaming current to flow with it. This flow of ions leads to a charge build-up in the downstream reservoir, inducing a back potential called streaming potential. Again, a current is generated in response to this streaming potential opposite to the streaming current, and it is called the conduction current. In the present work, we address the effect of counter flow induced by streaming potential on thermal characteristics of a non-Newtonian fluid with the consideration of asymmetric zeta potential and viscous dissipation. As high values of zeta potential are considered it would be erroneous to apply commonly assumed Boltzmann distribution. This is because the Boltzmann equation assumes charges to be point particles and will give an aphysically high density of charged particles in the vicinity of the wall. Therefore, for high zeta potentials, we need to take care of this finite size of the ions, also referred to as the 'steric effect'. The prime focus of the present work is to analyze, probably for the first time, the alterations in the associated thermal characteristics of ionic power-law fluid flows through closed narrow confinements having asymmetric zeta potentials, due to the induced streaming potential counter flow, while also considering the finite size of ions.

2. MATHEMATICAL FORMULATION

2.1. Problem definition and assumptions

We have considered solution flowing through a slit channel geometry with height $2H$, with origin at the lower wall of the slit; x represents the coordinate parallel to the walls while y represents the coordinate perpendicular to the walls. The surfaces are considered as electrically homogeneous which results in velocity having only one component parallel to the walls. For the estimation of fluid motion we have to consider the electrokinetic body force term, along with the pressure-gradient term and the viscous term. The next sub-section describes the ion-distribution and the potential profile associated with the EDL under the non-equilibrium conditions of fluid flow, though with some simplifications.

2.2. Electrokinetic description considering steric effects and asymmetric zeta potentials

The general species transport equation in a continuum model for a binary electrolyte with symmetric valences of the cation and the anion ($z_+ = -z_- = z$) in the steady state is: $\nabla \cdot \varphi_\pm = 0$. Here, $\varphi_\pm$ represents the flux of the cation and the anion. In the moderately dilute solution limit, this flux can be expressed in terms of the gradient of the electrochemical potential. In the moderately dilute solution limit, this flux can be expressed in terms of the gradient of the electrochemical potential $\mu_\pm$ as $\mathbf{j}_\pm = -m_\pm n_\pm \nabla \mu_\pm + n_\pm \mathbf{u}$ where $m_\pm$ is the ionic mobility, $n_\pm$ is the number density and $\mathbf{u}$ is the mean fluid velocity vector (with the axial direction component only). For a very dilute solution, $\mu_\pm$ can be written as $\mu_\pm = k_B T \ln n_\pm \pm ze\phi$, where k_B is the Boltzmann constant, T is the absolute temperature, e is the elementary charge and ϕ is the electric potential. A correction term is added in this equation to take care of finite size of ions (the Bikerman model) [6]

$$\mu_\pm = k_B T \ln n_\pm \pm ze\phi - k_B T \ln\left(1 - n_+ a^3 - n_- a^3\right) \tag{1}$$

where a is an effective molecular length scale. Then the expression of the flux becomes:

$$j_\pm = -D_\pm \left(\nabla n_\pm \pm \frac{ze}{k_B T} n_\pm \nabla\phi + \frac{n_\pm \nabla\left(n_+ + n_-\right) a^3}{1 - n_+ a^3 - n_- a^3} \right) + n_\pm \mathrm{u} \tag{2}$$

where $m_\pm = D_\pm / k_B T$, is the ionic mobility and $D_\pm$ is the ionic diffusivity. We also assume that $D_+ = D_- = D$. In addition to this, due to orthogonality of the flow direction and the direction of spatial arrangement of ions, non-equilibrium flow condition does not disturb the spatial structure of the distributions. This allows dividing the electric potential ϕ, into separate contributions from the screening potential ψ (associated with the ion distribution) and the streaming potential as $\phi(x, y) = \psi(y) - xE_s$, where E_s is the constant electric field associated with the streaming potential. Now applying $\nabla \cdot \varphi_\pm = 0$:

$$0 = D\frac{\partial^2 n_{\pm}}{\partial^2 y} \pm D\frac{ez}{k_B T}\frac{\partial}{\partial y}\left(n_{\pm}\frac{\partial \psi}{\partial y}\right) + Da^3\frac{\partial}{\partial y}\left\{\frac{n_{\pm}\left(\frac{\partial n_{+}}{\partial y}+\frac{\partial n_{-}}{\partial y}\right)}{1-(n_{+}+n_{-})a^3}\right\} \tag{3}$$

Integrating (3) once with respect to y and using the condition $\partial_y n_{\pm} = \partial_y \psi = 0$ we get:

$$0 = \frac{\partial \ln n_{+}}{\partial y} \pm \frac{ez}{k_B T}\left(\frac{\partial \psi}{\partial y}\right) - \frac{\partial}{\partial y}\left[\ln\left\{1-a^3\left(n_{+}+n_{-}\right)\right\}\right] \tag{4}$$

Again integrating Eq. (4) with respect to y and using the condition $n_{\pm} = n_0$ at $\psi = 0$ we get [5, 7-9]:

$$n_{\pm} = \frac{\exp\left(\mp\frac{ez\psi}{k_B T}\right)}{1-2n_0 a^3\left[1-\cosh\left(\frac{ez\psi}{k_B T}\right)\right]} \tag{5}$$

It should be noticed that to derive Eq. (5), no symmetry argument has been used. Therefore, difference in physio-chemical characteristics of two channel wall surface can be used in subsequent equations.

Now that we have the ionic distribution $n_{\pm}$ we can use it in the Poisson equation: $\partial_y^2 \psi = -\rho_e/\varepsilon$, where ε is the permittivity of the solvent (assumed constant here), and ρ_e is the charge density. After non-dimensionalizing the potential and the transverse coordinate by:

$$\bar{\psi} = \frac{\psi}{(k_B T/ez)} = \frac{ze\psi}{k_B T}; \bar{y} = \frac{y}{H} \tag{6}$$

We get:

$$\frac{\partial^2 \bar{\psi}}{\partial \bar{y}^2} = \kappa^2 \frac{\sinh\left(\bar{\psi}\right)}{1+2\nu\sinh^2\left(\bar{\psi}/2\right)}, \tag{7}$$

where $\kappa = H/\lambda$, with $\lambda = \sqrt{\varepsilon k_B T/2n_0 e^2 z^2}$ representing the Debye screening length, and ν representing the 'steric factor'. The boundary conditions used are:

$$\bar{\psi}\big|_{\bar{y}=0} = \bar{\xi}_B, \qquad \bar{\psi}\big|_{\bar{y}=2} = \bar{\xi}_T \tag{8}$$

Where $\bar{\xi}_B$ and $\bar{\xi}_T$ are the dimensionless zeta potentials at the bottom and the top wall respectively.

2.3. Momentum transport

Using Cauchy's equation for motion of fluid along x-direction as:

$$0 = -\frac{\partial p}{\partial x} + \frac{\partial \tau_{yx}}{\partial y} + F_{EK}, \tag{9}$$

where p is the pressure, τ_{yx} is the shear stress and $F_{EK} = \rho_e E_S = -\varepsilon\,\partial_y^2 \psi\, E_S$ is the electrokinetic body force term. Using the Ostwald–de Waele relationship [5, 10]:

$$\tau_{yx} = \eta \left| \frac{\partial u}{\partial y} \right|^{n-1} \frac{\partial u}{\partial y} \tag{10}$$

where η is the flow consistency index and n is the flow behavior index. Absolute values of the partial derivative are used to ensure real values of the shear stress magnitude. Upon replacing the mentioned expressions in Eq. (8) we obtain:

$$0 = -\frac{\partial p}{\partial x} + \frac{\partial}{\partial y}\left[\eta \left| \frac{\partial u}{\partial y} \right|^{n-1} \frac{\partial u}{\partial y} \right] - \varepsilon \frac{\partial^2 \psi}{\partial y^2} E_S \tag{11}$$

We use the following non-dimensionalization scheme [5, 10]:

$$\overline{u} = \frac{u}{U}, \quad \overline{E}_S = \frac{ezDE_S}{k_B TU} \tag{12}$$

Note that U is a reference velocity. We will discuss the expression for U in a short while. After suitable non-dimensionalizing of Eq. (11) using Equations (6) and (12) we arrive at the following momentum conservation equation:

$$0 = 1 + \frac{\partial}{\partial \overline{y}}\left[\left| \frac{\partial \overline{u}}{\partial \overline{y}} \right|^{n-1} \frac{\partial \overline{u}}{\partial \overline{y}} \right] - \overline{R} \frac{\partial^2 \overline{\psi}}{\partial \overline{y}^2} \overline{E}_S \tag{13}$$

It can be inferred from Eq. (13) that we have chosen U such that $\frac{\eta U^n}{H^{n+1}} = -\frac{\partial p}{\partial x}$, thus we have $\overline{R} = \left(\frac{H}{U} \right)^{n-1} \frac{\varepsilon k_B^2 T^2}{k e^2 z^2 D}$.

Integrating Eq. (13) with respect to $\overline{y}$ we obtain:

$$\left| \frac{\partial \overline{u}}{\partial \overline{y}} \right|^{n-1} \frac{\partial \overline{u}}{\partial \overline{y}} = -\overline{y} + \overline{R} \frac{\partial \overline{\psi}}{\partial \overline{y}} \overline{E}_S + c \ , \tag{14}$$

where c is the unknown constant of integration. In order to remove the modulus sign we can also write the equation as:

$$\frac{\partial \overline{u}}{\partial \overline{y}} = \begin{cases} \left[-\overline{y} + \overline{R} \frac{\partial \overline{\psi}}{\partial \overline{y}} \overline{E}_S + c \right]^{1/n}, & \frac{\partial \overline{u}}{\partial \overline{y}} \geq 0 \\ -\left[-\left\{ -\overline{y} + \overline{R} \frac{\partial \overline{\psi}}{\partial \overline{y}} \overline{E}_S + c \right\} \right]^{1/n}, & \frac{\partial \overline{u}}{\partial \overline{y}} < 0 \end{cases} \tag{15}$$

The velocity profile $\overline{u}$ in terms of $\overline{y}$ can be found out by $\overline{u} = \int_0^{\overline{y}} \left(\frac{\partial \overline{u}}{\partial \overline{y}} \right) dy$, though it should be noticed that values of both the constant of integration c and the streaming potential field E_S are still not known.

To determine E_S, we use the condition of zero ionic current across any general cross- section [4, 10]:

$$I_{ionic} = \int_0^{2H} ez\left(n_+u_+ - n_-u_-\right)dy + 2\sigma_{\text{Stern}}E_S = 0 \tag{16}$$

where $u_\pm = u \pm zeDE_S/k_BT$ are the cationic and the anionic velocities, and σ_{Stern} is the Stern layer conductivity. After non-dimensionalizing we get:

$$\overline{E}_S = \frac{I_1}{I_2 + 2Du}, \tag{17}$$

where,

$$I_1 = \int_0^2 \frac{\sinh\left(\overline{\psi}\right)}{1+2\nu\sinh^2\left(\overline{\psi}\right)}\overline{u}\ d\overline{y}; I_2 = \int_0^2 \frac{\cosh\left(\overline{\psi}\right)}{1+2\nu\sinh^2\left(\overline{\psi}\right)}\ d\overline{y} \tag{18}$$

And $Du = \dfrac{\sigma_{Stern}}{\sigma_b H}$ with $\sigma_b = \dfrac{n_0 e^2 z^2 D}{k_B T}$, is the Dukhin number. The complexity arising from the two unknowns c and $\overline{E}_S$ together with the implicit nature of the expression of $\overline{E}_S$ in Eq. (15) is addressed through an iterative numerical technique.

2.4. Thermal transport

Taking the viscous dissipation under consideration as well as assuming only axial flow and constant fluid properties, the energy equation can be written as:

$$\rho c_P u\frac{\partial T}{\partial x} = k\left(\frac{\partial^2 T}{\partial x^2} + \frac{\partial^2 T}{\partial y^2}\right) + \tau_{xy}\left(\frac{\partial u}{\partial y}\right) \tag{19}$$

where ρ is the density of the fluid, c_p is the specific heat capacity at constant pressure, T is the temperature of the fluid, and k is the thermal conductivity. For a thermally fully developed flow with constant flux boundary condition it can be easily proved that [11]:

$$\frac{\partial T}{\partial x} = \frac{dT_W}{dx} = \frac{dT_M}{dx} = \text{Constant} \tag{20}$$

This shows that $\partial^2 T/\partial x^2 = 0$; therefore for a thermally fully developed flow with constant heat flux boundary condition the axial conduction term is zero. Now applying energy balance in a control volume of length dx with no internal heat source [12]:

$$(2H\rho u_a)c_p\left\{\left(T_M + dT_M\right) - T_M\right\} = (q_B'' + q_T'' + \int_0^{2H}\eta\left|\frac{du}{dy}\right|^{n+1}dy)dx \tag{21}$$

$$\Rightarrow (2H\rho u_a)c_p\left(\frac{dT_M}{dx}\right) = q_B'' + q_T'' + \int_0^{2H}\eta\left(\frac{du}{dy}\right)^{n+1}dy, \tag{22}$$

where u_a is the average flow velocity, q_B'' and q_T'' are constant heat fluxes through the bottom wall and the top wall respectively. Substituting Eq. (22) and Eq. (20) in Eq. (19) and non-dimensionalising we get:

$$\frac{d^2\theta}{d\bar{y}^2} = \frac{u_0}{2}\left[1 + q_r'' + G\left\{\int_0^2 \left(\frac{d\bar{u}}{d\bar{y}}\right)^{n+1} d\bar{y}\right\}\right] - G\left(\frac{d\bar{u}}{d\bar{y}}\right) \tag{23}$$

Here, $u_0 = \frac{u}{u_a}$, $q_r'' = \frac{q_T''}{q_B''}$, $\theta = \left(\frac{T - T_{W,b}}{q''_B H/k}\right)$ and $G = \frac{\eta U^{n+1}}{q_B'' H^n}$ can be treated as the viscous dissipation parameter which is usually referred to as the modified Brinkmann number in case of non-Newtonian flows. Note that $T_{W,b}$ is the temperature of the bottom plate. Equation (23) can be solved subject to the following boundary conditions:

$$\theta\big|_{\bar{y}=0} = 0; \qquad \left.\frac{\partial\theta}{\partial\bar{y}}\right|_{\bar{y}=2} = q_r'' \tag{24}$$

In the subsequent section non-dimensionalised temperature and velocity profiles have been plotted after numerically solving the equations (15) and (23), with the variations in 'steric factor' ν, flow behavior index n, non-dimensional Debye length κ and the non-dimensional potentials at the two walls $\bar{\zeta}_T$ and $\bar{\zeta}_B$.

3. RESULTS AND DISCUSSIONS

The alterations in the velocity profile and the non-dimensional temperature distribution, triggered by the variations in the streaming field induced advective transport due to the increasing asymmetry in the wall ζ-potentials, is exhibited in Fig. 1 for Newtonian fluids ($n = 1$) by considering the steric effect of ions ($\nu = 0.2$), for $\kappa = 5$.

Note that for Fig. 1 the flux ratio $q_r'' = 1$ i.e. the top wall and the bottom wall are both subjected to fluxes of equal magnitude. The increase in asymmetry in the values of the non-dimensional ζ-potentials also leads to an increase in the asymmetry of the velocity profile, as is evident from Fig. 1(a). As explained earlier, the development of ζ-potentials and the associated electrokinetic effects generate a streaming field E_S in the direction opposite to the favorable pressure gradient which triggers a 'back flow' that hinders the actual pressure-driven flow of the fluid. Greater the magnitude of the ζ-potential, greater will be the back flow induced [5, 7]. This is due to a dense stacking up of the counter-ions near the walls as a result of higher wall potential, which in turn provides enhanced back-flow due to the streaming potential field E_S. The counter-flow of ions then drags the bulk fluid along with it, thus generating significant back-flow. We observe a symmetrical distribution of velocity for the case of identical ζ-potentials at both the surfaces and this symmetry is disturbed as the ζ-potential at the top wall is changed. The velocity curve tends to shift towards the side having lesser ζ-potential, which in this case is the bottom surface ($\bar{y} = 0$ is the bottom surface and $\bar{y} = 2$, the top surface). This is understandable, as the fluid will encounter more resistance in the vicinity of the wall having greater ζ-potential. Interestingly, if the ζ-potential is high enough one may come across a situation wherein the fluid elements tend to move in the opposite direction of the favorable pressure gradient i.e. there may be a negative value of the fluid velocity at some points. This situation is demonstrated to an extent for the case of $\bar{\zeta}_B = -1$; $\bar{\zeta}_T = -4$ in Fig. 1(a). In Fig.1(b) we can see that with increasing asymmetry, we have an increasing temperature of the fluid near the top wall $\bar{y} = 2$ i.e. the non-dimensional temperature θ at the top wall is increasing from zero and becoming more and more positive with increasing values of ζ-potential at the top surface. From the definition of θ given previously, we infer that the temperature at the top wall is exceeding that of the bottom surface. This can be explained by keeping in mind that we have same inward flux at both the surfaces. This flux can be represented in terms of the heat transfer coefficient as $q''_{W,\,b/t} = h_{b/t}(T_{W,\,b/t} - T_m)$, where subscripts b/t represent the relevant values at the bottom/top surfaces respectively and T_M is the mean bulk fluid temperature. Now, as the average fluid velocity is lesser for the top half of the channel (on account of greater ζ-potential), the effective heat transfer coefficient will be lesser for the top surface than that of the bottom surface and hence it has a higher temperature, in order to preserve the value of heat flux which is same for both surfaces $\bar{y} = 0$ and $\bar{y} = 2$.

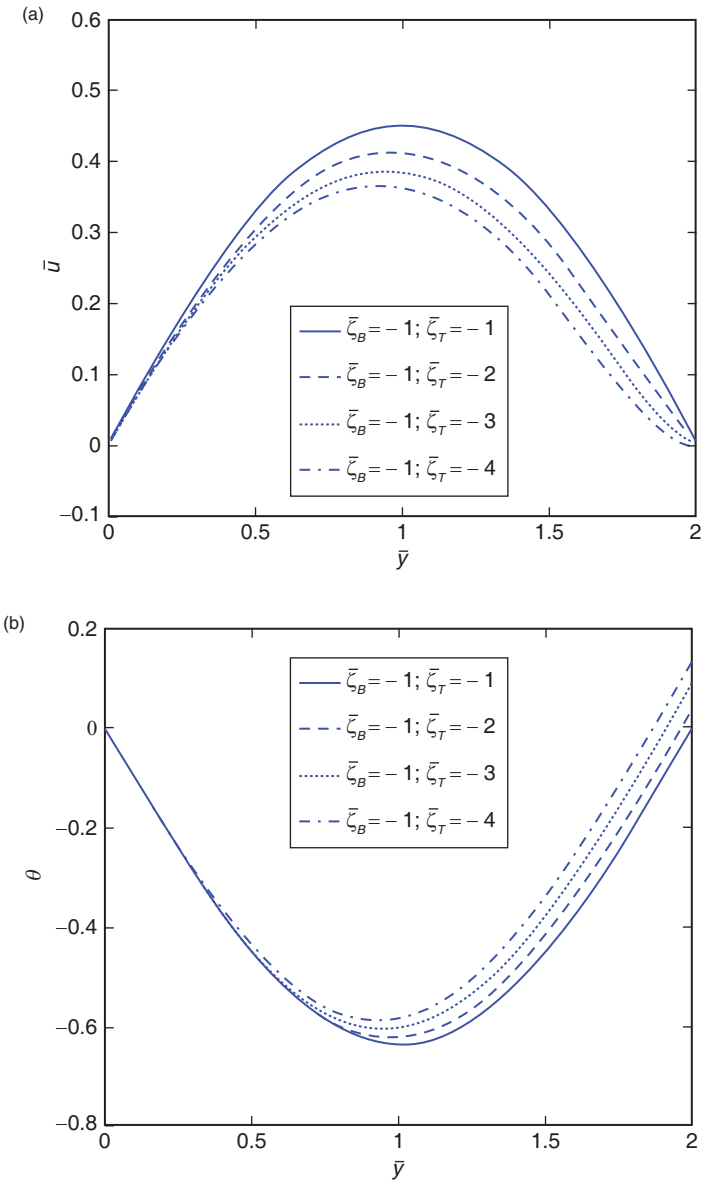

Figure 1. (a) Variations in the cross-sectional flow velocity distribution (b) Variations in the non-dimensional temperature distribution, with increasing asymmetry in the wall ζ-potentials for finite ionic sizes, with $\nu = 0.2$, $\kappa = 5$, $n = 1$, $q_r'' = 1$

From Figure 2(a) we can conclude that for $n<1$ the average velocity of the fluid is minimum, while it is maximum for $n>1$. A Newtonian fluid's ($n=1$) behavior, of course, lies intermediate to these two fluids. This means that, all other factors being constant, the effective viscosity of a pseudoplastic fluid ($n<1$) is greater than that of a dilatant fluid ($n>1$). Thus a pseudoplastic fluid is most resistant to the pressure-driven flow, followed by a Newtonian fluid and a dilatant fluid offers least resistance to the pressure gradient. A comparison of the effective viscosities of the three fluids under consideration also explains the nature of the temperature profiles in the three cases (Fig. 2(b)). As is evident from the energy equation (19), the term $\tau_{xy}(\partial u/\partial y)$ represents the viscous dissipation due to viscous interaction between the fluid layers. This viscous dissipation is actually the mechanical energy lost by the fluid and

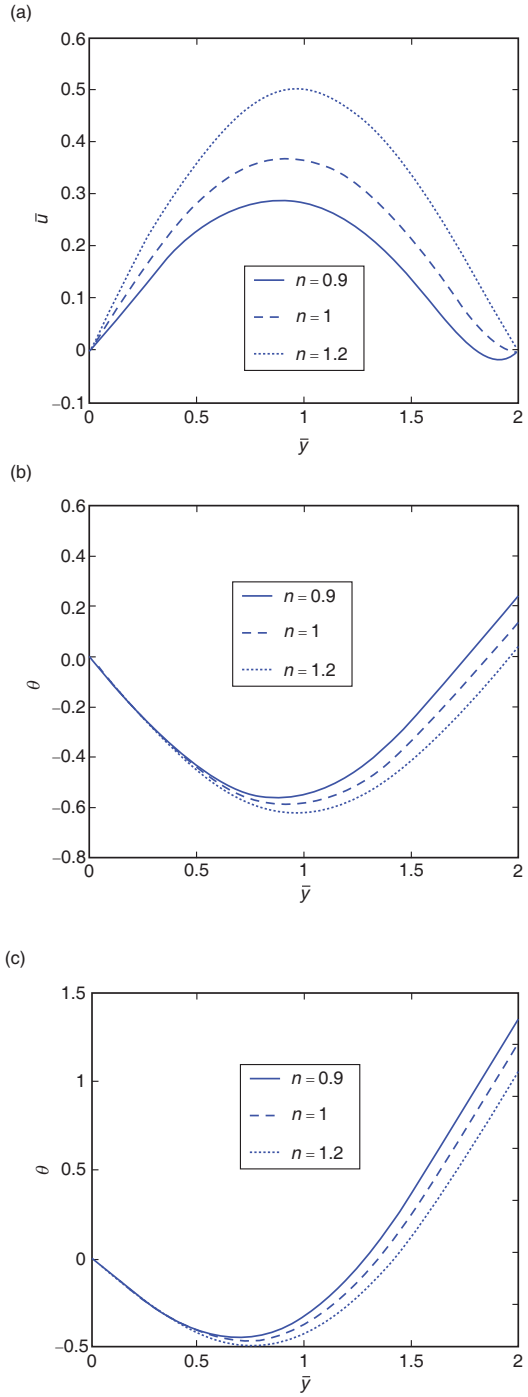

Figure 2. (a) Variations in the cross-sectional flow velocity distribution for different fluids (b),(c) Variations in the non-dimensional temperature distribution, for different fluids for finite ionic sizes, with $\nu = 0.2$, $\kappa = 5$, $\bar{\xi}_B = -1$; $\bar{\xi}_T = -4$, (b) $q_r'' = 1$ and (c) $q_r'' = 2$

is responsible for an increase in the average temperature of the fluid. In other words, it acts as a source term in the energy equation. Naturally, for $n = 0.9$, the viscous dissipation is the highest due to its greater apparent viscosity. Thus, for a pseudoplastic fluid the average temperature is higher than that of a Newtonian fluid, which in turn is greater than that of a dilatant fluid. The asymmetry introduced by the different values of ζ-potentials is also evident and can be explained as mentioned before.

Introducing different heat fluxes through the two walls further magnifies the asymmetry, with the temperatures at the top surface being significantly higher than those at the bottom as can be seen clearly in Fig. 2(c).

For very high ζ-potentials, the consideration of point-sized ions ($\nu = 0$) leads to an infinitely large concentration of counter-ions near the surface. It is to overcome this unrealistic situation that the Bikerman model for the electrochemical potential given by Eqn. (1) is adopted and the potential distribution is calculated after considering the modified charge distribution given by Eqn. (5). We now investigate the effect of having finite sized ions, the size of which is indicated by the parameter ν. Higher the value of ν, greater is the size of the ions under consideration. From the velocity distribution plots of Fig. 3(a) we infer that larger ions (higher value of ν) tend to inhibit fluid flow in micro-channels to a greater extent. Higher value of the 'steric factor' leads to an increase in the extent to which the counterions are "stacked up" against the wall to effectively screen the high surface charge. It is this stacking up of the counterions which leads to a stronger conductive response to the induced streaming potential field, and, consequently, a stronger back-flow of the fluid. Even for the same value of the steric factor, a higher magnitude of the zeta potential again leads to an increase in the extent of the "stacked up" counterions. Thus, this too leads to a higher back-flow situation, as manifested in the Fig. 1(a). It is this higher back-flow which influences the temperature profiles too, both in value and asymmetry.

Again in Fig. 3(a) we see the extent to which back-flow is induced by the streaming potential field for $\nu = 0.04$, where the fluid has significant negative velocity in the vicinity of the top wall. Thus, one can infer straight away that the ζ-potential is greater for the top surface, which is indeed the case here ($\bar{\zeta}_B = -4$; $\bar{\zeta}_T = -8$). Note that even though the ζ-potential values are same for both cases of $\nu = 0.04$ and $\nu = 0.4$, there exists greater asymmetry for the latter case as compared to the former. This leads to a very important conclusion, namely, increasing the size of ions (by changing the solute) while maintaining a certain asymmetry in ζ-potential values tends to further disturb the symmetry of the system. As the momentum conservation equation (9) and the thermal transport equation (19) are coupled through the velocity u of the fluid, asymmetries in the velocity profiles of Fig. 3(a) automatically get reflected in the corresponding thermal plots of θ vs $\bar{y}$ in Fig. 3(b).

4. SUMMARY AND CONCLUSIONS

In the present study we analyzed the effects of various factors of electrokinetics (like asymmetry in the values of ζ-potentials at the top and bottom surfaces of a micro-channel, a finite ion-size consideration) on the velocity and the temperature profiles of a one-dimensional, pressure-driven, streaming potential flow in a parallel plate micro-channel. The consideration of finite ion-size, also known as the 'steric effect' is modeled using the Bikerman model of electrochemical potential distribution, in order to avoid the unrealistically high values of the counter-ion concentration near the charged surfaces predicted by the traditional Poisson-Boltzmann formalism. These uncharacteristically high values are mainly obtained for correspondingly high values of the ζ-potentials, the very regime where streaming potential effects are the strongest. The velocity and the temperature fields were non-dimensionalised using suitable references and their behaviour under different conditions was examined by varying certain tunable parameters like wall ζ-potentials or by changing the fluid nature (considering dilatant or pseudoplastic fluids) or by altering the appropriate bulk volume fraction of ions (the parameter ν). The intuition of a disruption in symmetry was confirmed for the case of asymmetric ζ-potentials and it was observed that this asymmetry was in direct proportion to the degree of asymmetry in the values of the ζ-potentials. The cause behind this was attributed to the fact that higher ζ-potentials meant a progressively increasing extent of stacking up of ions near the surfaces, which also resulted in increased

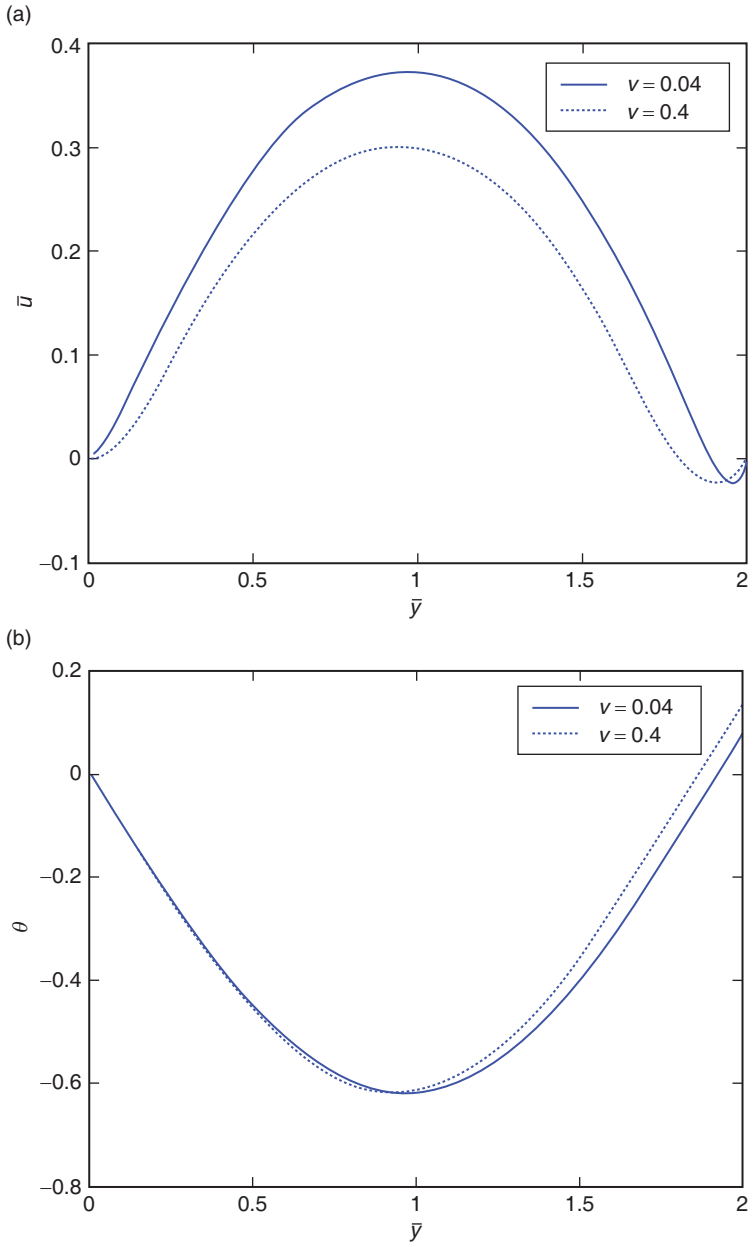

Figure 3. (a) Variations in the cross-sectional flow velocity distribution for different values of 'steric factor' ν (b) Variations in the non-dimensional temperature distribution, for different values of 'steric factor'ν, with $n = 0.9$, $\kappa = 10$, $\bar{\zeta}_B = -4$; $\bar{\zeta}_T = -8$, $q_r'' = 1$

back-flow due to the induced streaming potential field E_S. The asymmetry in the velocities was reflected in that of the temperature profiles on account of different local heat transfer coefficients. This difference regardless of the condition of equal heat flux 'entering' the channel from the two surfaces meant that there was an asymmetry in the temperature plots. The surface with higher ζ-potential had lower fluid velocity in its vicinity, leading to lower heat transfer coefficient and consequently a higher wall temperature. It was also noted that as the effective viscosity increases, the average fluid velocity

decreases and thus for fluids with higher flow behavior index n (lower effective viscosity), higher values of average velocities were observed. The effective viscosity also governed the average temperature of the fluid, with greater values of n (meaning lesser values of effective viscosity) culminating into lesser average temperatures. This dependence manifested in the form of the viscous dissipation term that increases with increasing values of effective viscosity. The observations for varying values of the 'steric factor' ν suggest that increasing values of ν lead to increased back-flow on account of more prominent stacking up of ions that get conducted in the direction of the streaming potential field E_S, as explained earlier. In addition to this, it was also seen that the asymmetry is enhanced as the 'steric factor' ν increases, but only if there pre-exists some asymmetry on account of disparate values of the ζ-potentials. These asymmetries in the velocity profiles get duly reflected in the temperature plots too as a consequence of the coupling of the momentum and the energy equations through the velocity field.

We expect that the theoretical framework presented in this study will provide a systematic basis for designing practical devices that exploit electrokinetic influences for tuning fluidic transport. On a more futuristic note, the present study may be considered to be a key step forward towards more sophisticated models of non-isothermal flows influenced by a number of other effects that work in close cohesion with streaming potential effects. Further progress would entail the consideration of the non-isothermal effects on the fluid flow, species transport and thermal characteristics in a truly coupled way.

REFERENCES

[1] S. Chakraborty, in: D. Li (Ed.), *Encyclopedia of Microfluidics and Nanofluidics*, Springer, New York, 2008, 444–453.

[2] D. Li, *Electrokinetics in Microfluidics*. Elsevier, London, 2004.

[3] R.J. Hunter, *Foundations of Colloid Science*. Oxford University Press, New York, 2001.

[4] J. Chakraborty, S. Chakraborty, in: S. Chakraborty (Ed.), *Mechanics Over Micro and Nano Scales*, Springer, New York, 2011, 1–60.

[5] R. Dey, J. Chakraborty, S. Chakraborty, Combined Interplay Of Steric Effects And Asymmetric Zeta Potential On Electrokinetic Transport Of Non-Newtonian Fluids Through Narrow Confinements: Studies On Streaming Potential. *Proceedings of the 3rd European Conference on Microfluidics* – Microfluidics – 2012 – Heidelberg. Dec. 3–5, 2012. Paper ID: μ FLU12-60.

[6] J.J. Bikerman, Structure and capacity of the electrical double layer, *Philosophical Magazine*, **33(220)**, 1942, 384–97.

[7] A.S. Khair, T.M. Squires, Ion steric effects on electrophoresis of a colloidal particle, *J. Fluid Mech.*, **640**, 2009, 342–356.

[8] A. Shenoy, J. Chakraborty, S. Chakraborty, Influence of streaming potential on pulsatile pressure-gradient driven flow through an annulus, *Electrophoresis*, **34**, 2013, 691–699.

[9] J. Chakraborty, R. Dey, S. Chakraborty, Consistent accounting of steric effects for prediction of streaming potential in narrow confinements, *Phys. Rev. E*, **86**, 2012, 061504-1-061504-5.

[10] R. Dey, J. Chakraborty, S. Chakraborty, Heat Transfer Characteristics of Non-Newtonian Fluid Flows in Narrow Confinements Considering the Effects of Streaming Potential, *International Journal of Micro-Nano Scale Transport*, **4**, 2011, 259–268.

[11] F.P. Incropera, D.P De Witt, *Fundamentals of Heat and Mass Transfer*. John Wiley & Sons, New York, 2002.

[12] C.Y. Soong, S.H. Wang, Theoretical analysis of electrokinetic flow and heat transfer in a microchannel under asymmetric boundary conditions, *J. Colloid Interface Sci.*, **265**, 2003, 202–213.